

1

2 Supporting Information for

3 Ionic Peltier Effect in Li-Ion Electrolytes

4 Zhe Cheng, Yu-Ju Huang, Benjamin Zahiri, Patrick Kwon, Paul V. Braun, David G. Cahill

5 E-mail: d-cahill@illinois.edu

6 This PDF file includes:

7 Figs. S1 to S8

8 Tables S1 to S7

9 SI References

10 **Heading**

11 **Note for Fig. S5.** The electrode potential temperature coefficients of closely related liquid electrolytes (LiTFSI-DOL-DME and
12 LiPF₆-EC-DEC) were obtained by Wang and co-workers (1) by imposing a temperature difference between two electrodes
13 and measuring the resulting open circuit voltage. The electrode potential temperature coefficients are equivalent to the ionic
14 Seebeck coefficients of the cell. We use the Onsager relation to calculate the corresponding ionic Peltier coefficient from the
15 data of Ref. (1) and compare the measurements of Ref. (1) to our measurements in Fig. S5.

16 **Determination of thermal conductivity of composite by effective medium theory.** For a separator of randomly-oriented glass
17 fibers with volume fraction f and thermal conductivity Λ_g embedded in a liquid electrolyte matrix with thermal conductivity
18 Λ_m , the analysis of Ref. (2) gives the following effective medium thermal conductivity Λ^* for the separator/liquid-electrolyte
19 composite:

20
$$\beta_1 = 2 \frac{\Lambda_g - \Lambda_m}{\Lambda_g + \Lambda_m} \quad [S1]$$

21
$$\beta_2 = \frac{\Lambda_g - \Lambda_m}{\Lambda_m} \quad [S2]$$

22
$$\Lambda^* = \Lambda_m \frac{3 + f(\beta_1 + \beta_2)}{3 - f\beta_1} \quad [S3]$$

23 For typical combinations of Λ_g , Λ_m , and f that we encountered in our work, the prediction of Eq. S3 is approximately 10%
24 larger than the prediction of the Landauer symmetric theory, and nearly identical to the average of the Hashin-Shtrikman
25 upper and lower bounds on the conductivity of an isotropic composite.

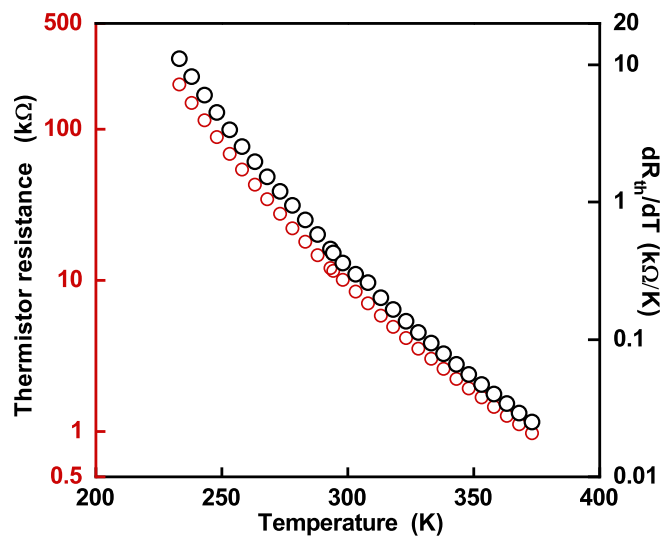


Fig. S1. Temperature dependent electrical resistance (R_{th}) and dR_{th}/dT of thermistors. The red circles are data for $R_{th}(T)$ provided by the manufacturer of the thermistor. The black circles are calculated values of dR_{th}/dT obtained by taking the derivative of a polynomial fit to R_{th} .

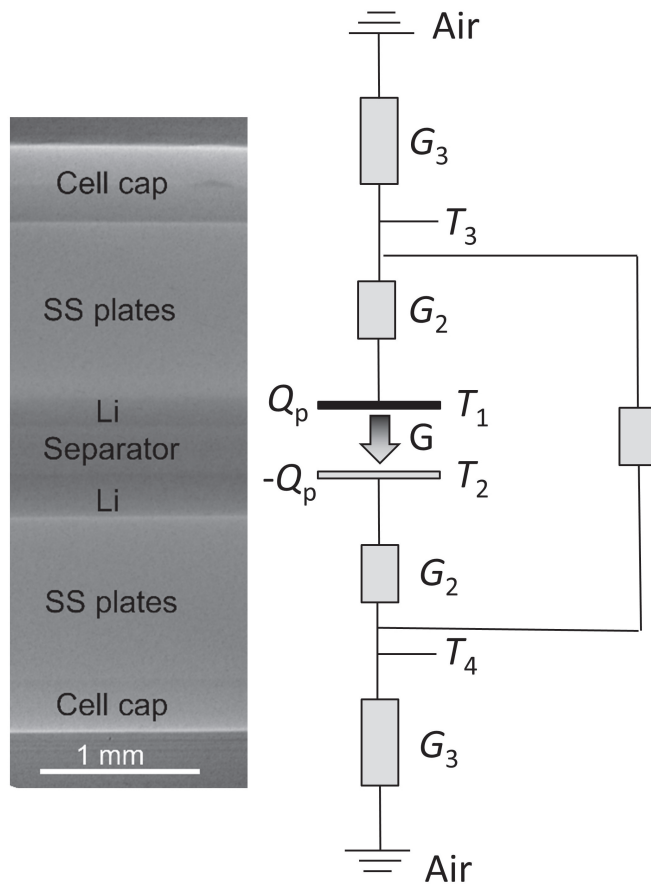


Fig. S2. The left panel a the cross-sectional image of the central section of a coin cell from x-ray computed tomography (CT). The right panel is the schematic of the thermal resistance network of the coin cell. The thermal conductance G of the separator/liquid-electrolyte composite is much larger than G_3 . The heat conduction through the rubber O-ring sandwiched by the cell caps (Grubber) is also included in the thermal resistance network.

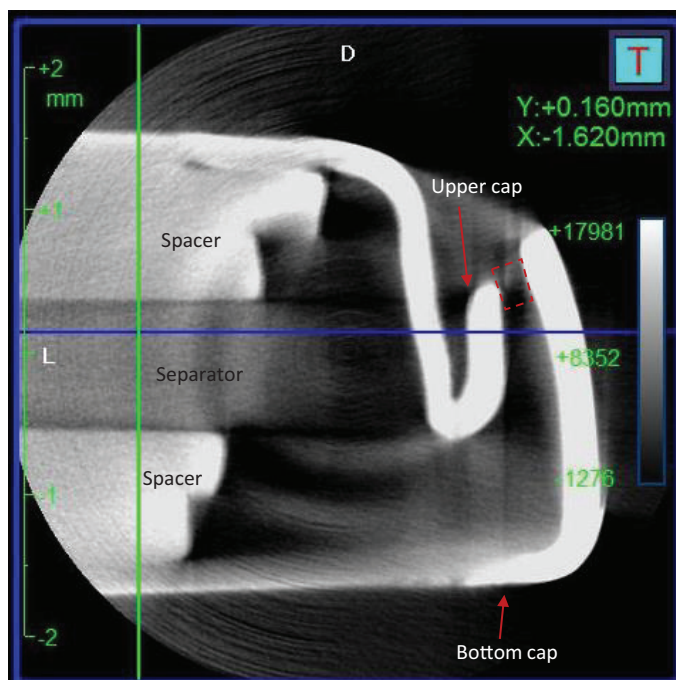


Fig. S3. Cross-sectional image of the edge of the coin cell from x-ray computed tomography (CT). The small rectangle outlined in a red dash line shows where the rubber O-ring rubber. The green and blue lines are the location of the mouse and the green numbers show the coordinates. The contact area of the two caps which sandwich a layer of the rubber sealing O-ring is approximately 10% of the separator area of the coin cell. The estimated thermal conductance of the O-ring contact between the upper and bottom cap is 15 mW K^{-1} , approximately 10% of the thermal conductance of the separator/liquid-electrolyte composite.

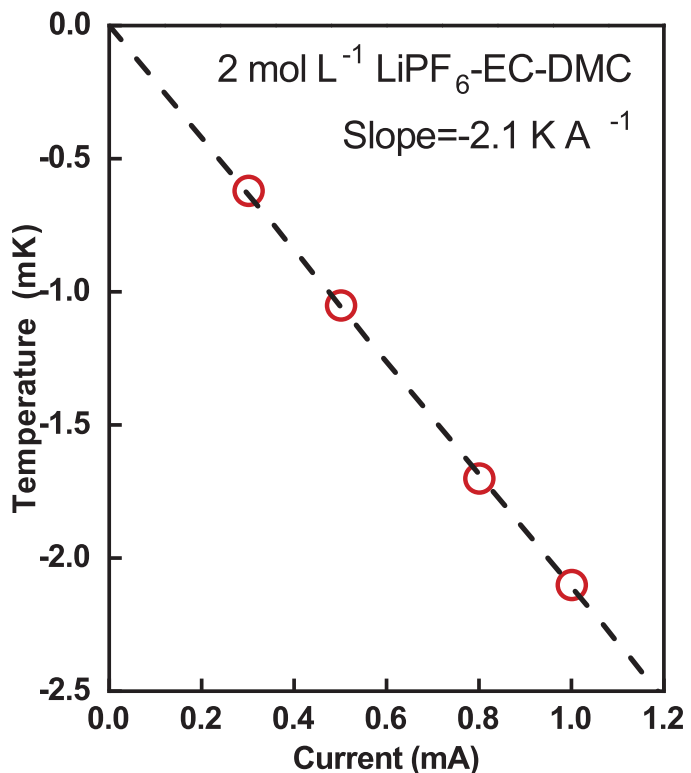


Fig. S4. Red circles are measurements of the temperature difference responses of a coin cell with 2 mol L^{-1} LiPF₆-EC-DMC liquid electrolyte as a function of applied currents. The fit to a linear relationship with zero intercept is depicted by the dashed line. The slope of this line is -2.1 K A^{-1}

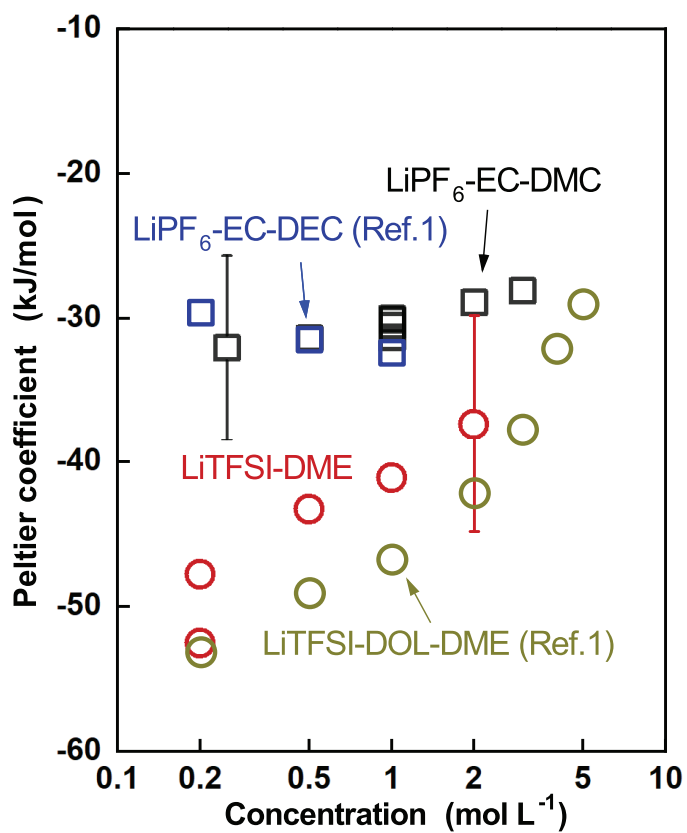


Fig. S5. The Peltier coefficients of liquid electrolytes measured in this work (red circles, LiTFSI-DME and black squares, LiPF₆-EC-DMC) are compared with the Peltier coefficients calculated from applying the Onsager relationship to electrode potential temperature coefficient of closely related liquid electrolytes (green circles, LiTFSI-DOL-DME and blue squares, LiPF₆-EC-DEC) obtained by imposing a temperature difference and measuring the voltage difference(1).

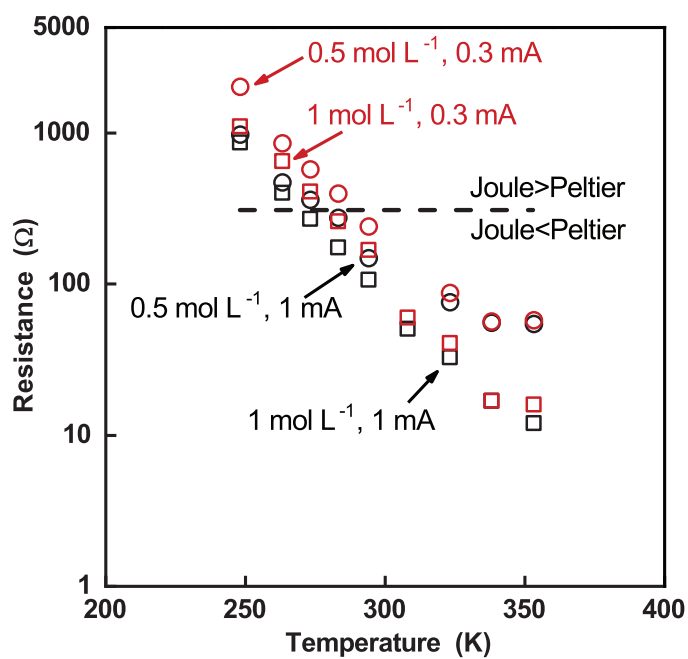


Fig. S6. Temperature dependent resistances of symmetric coin cells with 0.5 mol L^{-1} and 1 mol L^{-1} $\text{LiPF}_6\text{-EC-DMC}$ liquid electrolytes. The dash line depicts the resistance at which the ionic Peltier heat is approximately equal to the Joule heat.

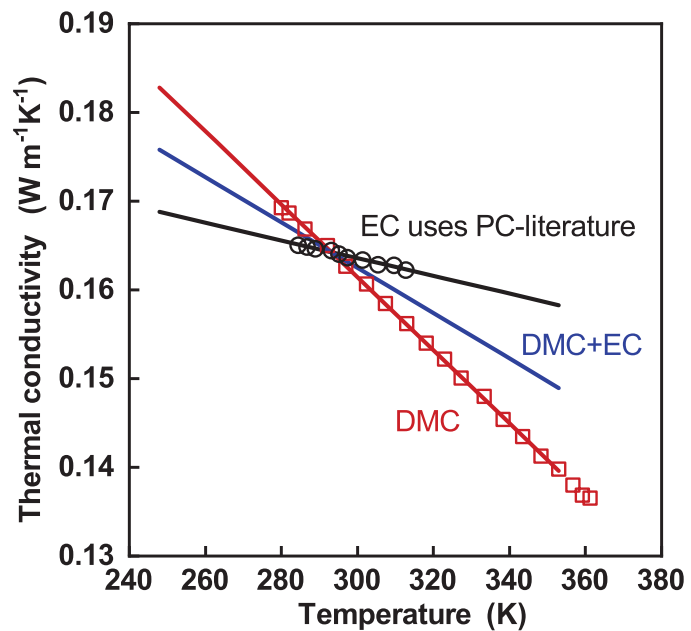


Fig. S7. Temperature dependence of the thermal conductivity of solvents in the electrolytes. The symbols are experimental thermal conductivity data from the literature (3–5). We use linear extrapolations to obtain data points which are not available for a specific temperature. The thermal conductivity data of ethylene carbonate (EC) is not available in the literature and we therefore use data of the structurally-similar propylene carbonate (PC). DMC is dimethyl carbonate. The temperature-dependent thermal conductivity of EC and DMC are used in Table S1 to S7 for the calculation of Peltier coefficient.

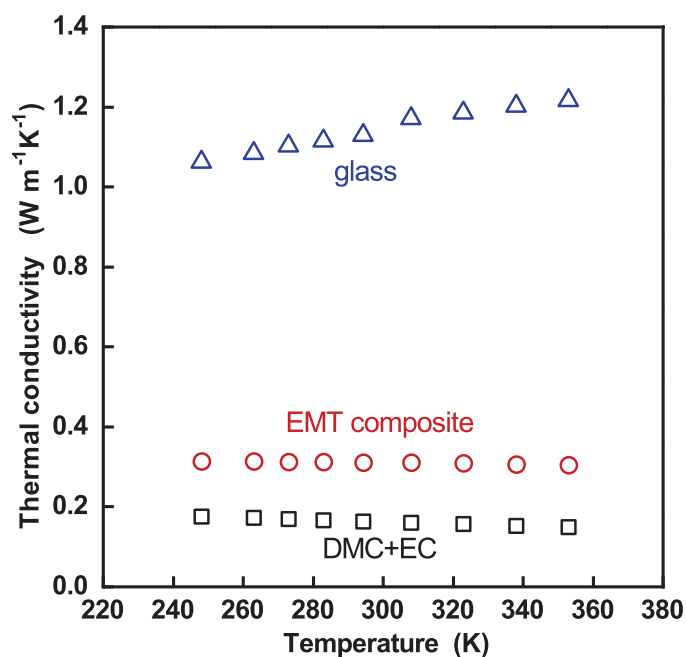


Fig. S8. Temperature-dependent thermal conductivity of the separator/liquid-electrolyte composite calculated by effective medium theory (EMT) using equation 23 of Ref. (2). See note on page 2 of SI for the calculation of the thermal conductivity of the composite. The thermal conductivity of borosilicate glass fiber is taken from the literature (6).

Table S1. Coin cell fabrication, calculated separator/liquid-electrolyte thermal conductivity (Λ^* defined by Eq. S3), and Peltier coefficient at 294.3 K. Slope is the slope of the temperature difference response as a function of applied current, as shown in Fig. S4.

Electrolyte	Salt concentration (mol L ⁻¹)	Amount of separator layers	Separator volume (mm ³)	Composite thickness (μm)	Composite volume (mm ³)	Separator volume fraction f	Composite Λ^* (W/m ² K))	Conductance G (mW/K)	Slope (mK/mA)	Peltier coefficient II (kJ/mol)
LiTFSI-DME	0.2	2	21.1	308	61.9	0.34	0.35	236	-2.31	-52.5
LiTFSI-DME	0.2	2	21.1	350	70.4	0.3	0.32	190	-2.6	-47.8
LiTFSI-DME	0.5	1	10.4	304	61.1	0.17	0.24	164	-2.74	-43.3
LiTFSI-DME	1	1	10.4	277	55.7	0.19	0.25	187	-2.28	-41.1
LiTFSI-DME	2	1	10.4	365	73.4	0.14	0.22	127	-3.05	-37.3
LiPF ₆ -DMC	1	2	21.1	475	95.5	0.22	0.28	126	-2.6	-31.6
LiPF ₆ -DMC	1	2	21.1	505	102	0.21	0.28	115	-2.77	-30.7
LiPF ₆ -EC-DMC	0.25	2	20.8	408	82.0	0.25	0.30	157	-2.11	-32.0
LiPF ₆ -EC-DMC	0.5	2	20.8	432	86.9	0.24	0.30	144	-2.26	-31.4
LiPF ₆ -EC-DMC	1	2	20.8	394	79.2	0.26	0.31	166	-1.88	-30.1
LiPF ₆ -EC-DMC	1	2	21.1	485	97.5	0.22	0.28	122	-2.64	-31.1
LiPF ₆ -EC-DMC (LCO)	1	2	20.8	585	118	0.18	0.26	93	-3.41	-30.5
LiPF ₆ -EC-DMC	2	1	10.4	355	71.4	0.15	0.24	142	-2.11	-28.9
LiPF ₆ -EC-DMC	3	2	21.1	525	106	0.2	0.27	109	-2.68	-28.1

Table S2. Glass fiber thermal conductivity, electrolyte thermal conductivity, β_1 , and β_2 at 294.3 K. (β_1 and β_2 are defined by Eq. S1 and S2, respectively.)

Electrolyte	Glass fiber Λ_g (W/(m*K))	Electrolyte Λ_m (W/(m*K))	β_1	β_2
LiTFSI-DME	1.13	0.15	1.54	6.67
LiPF ₆ -EC-DMC	1.13	0.16	1.49	5.89

Table S3. Temperature dependent ionic Peltier coefficients of 1 mol L⁻¹ LiPF6-EC-DMC. (β_1 and β_2 are defined by Eq. S1 and S2, respectively. Λ^* is defined by Eq. S3.)

Temperature	Glass fiber Λ_g	Electrolyte Λ_m	β_1	β_2	Composite Λ^*	Conductance G (mW/K)	Slope (mK/mA)	Peltier coefficient II (kJ/mol)
248	1.06	0.18	1.43	5.04	0.31	168	-1.73	-28.1
263	1.08	0.17	1.45	5.30	0.31	167	-1.79	-29.0
273	1.10	0.17	1.47	5.51	0.31	167	-1.74	-28.1
283	1.12	0.17	1.48	5.69	0.31	166	-1.73	-27.8
294.3	1.13	0.16	1.49	5.89	0.31	166	-1.88	-30.1
308	1.17	0.16	1.52	6.30	0.31	166	-1.87	-30.0
323	1.19	0.16	1.53	6.57	0.31	165	-2.08	-33.1
338	1.20	0.15	1.55	6.87	0.31	164	-2.31	-36.6
353	1.22	0.15	1.56	7.16	0.30	162	-2.45	-38.3

Table S4. Temperature dependent ionic Peltier coefficients of 0.5 mol L⁻¹ LiPF6-EC-DMC (cell-1). (β_1 and β_2 are defined by Eq. S1 and S2, respectively. Λ^* is defined by Eq. S3.)

Temperature	Glass fiber Λ_g	Electrolyte Λ_m	β_1	β_2	Composite Λ^*	Conductance G (mW/K)	Slope (mK/mA)	Peltier coefficient II (kJ/mol)
248	1.06	0.18	1.43	5.04	0.34	208	-1.65	-33.1
263	1.08	0.17	1.45	5.30	0.34	207	-1.60	-32.1
273	1.10	0.17	1.47	5.51	0.34	207	-1.62	-32.3
283	1.12	0.17	1.48	5.69	0.34	207	-1.64	-32.7
294.3	1.13	0.16	1.49	5.89	0.34	206	-1.61	-32.0
308	1.17	0.16	1.52	6.30	0.34	207	-1.59	-31.7
323	1.19	0.16	1.53	6.57	0.34	206	-1.77	-35.1
338	1.20	0.15	1.55	6.87	0.33	205	-1.97	-38.9
353	1.22	0.15	1.56	7.16	0.33	203	-2.07	-40.6

Table S5. Temperature dependent ionic Peltier coefficients of 0.5 mol L⁻¹ LiPF6-EC-DMC (cell-2). Cell failed at T > 294.3 K. (β_1 and β_2 are defined by Eq. S1 and S2, respectively. Λ^* is defined by Eq. S3.)

Temperature	Glass fiber Λ_g	Electrolyte Λ_m	β_1	β_2	Composite Λ^*	Conductance G (mW/K)	Slope (mK/mA)	Peltier coefficient II (kJ/mol)
263	1.08	0.17	1.45	5.30	0.30	146	-2.07	-29.2
273	1.10	0.17	1.47	5.51	0.30	145	-1.99	-27.9
283	1.12	0.17	1.48	5.69	0.30	145	-2.07	-29.0
294.3	1.13	0.16	1.49	5.89	0.30	144	-2.26	-31.4

Table S6. Temperature dependent ionic Peltier coefficients of 1 mol L⁻¹ LiPF6-DMC (cell-1). (β_1 and β_2 are defined by Eq. S1 and S2, respectively. Λ^* is defined by Eq. S3.)

Temperature	Glass fiber Λ_g	Electrolyte Λ_m	β_1	β_2	Composite Λ^*	Conductance G (mW/K)	Slope (mK/mA)	Peltier coefficient Π (kJ/mol)
283	1.12	0.17	1.48	5.63	0.29	127	-2.65	-32.6
295	1.13	0.16	1.49	5.90	0.28	126	-2.6	-31.6
308	1.17	0.16	1.52	6.41	0.28	125	-2.76	-33.3
323	1.19	0.15	1.55	6.80	0.28	123	-2.99	-35.4
338	1.20	0.15	1.57	7.24	0.27	120	-3.06	-35.5

Table S7. Temperature dependent ionic Peltier coefficients of 1 mol L⁻¹ LiPF6-DMC (cell-2). (β_1 and β_2 are defined by Eq. S1 and S2, respectively. Λ^* is defined by Eq. S3.)

Temperature	Glass fiber Λ_g	Electrolyte Λ_m	β_1	β_2	Composite Λ^*	Conductance G (mW/K)	Slope (mK/mA)	Peltier coefficient II (kJ/mol)
283.1	1.12	0.17	1.48	5.63	0.280	116	-2.6	-29.2
295	1.13	0.16	1.49	5.90	0.276	115	-2.77	-30.7
307.6	1.17	0.16	1.52	6.41	0.274	114	-3.05	-33.6
333.5	1.20	0.15	1.57	7.24	0.264	110	-3.3	-34.9

28 **References**

- 29 1. H Wang, et al., Correlating Li-ion solvation structures and electrode potential temperature coefficients. *J. Am. Chem. Soc.*
30 **143**, 2264–2271 (2021).
- 31 2. CW Nan, R Birringer, DR Clarke, H Gleiter, Effective thermal conductivity of particulate composites with interfacial
32 thermal resistance. *J. Appl. Phys.* **81**, 6692–6699 (1997).
- 33 3. X Jin, J Wu, Z Liu, J Pan, The thermal conductivity of dimethyl carbonate in the liquid phase. *Fluid Phase Equilibria*
34 **220**, 37–40 (2004).
- 35 4. M Tuliszka, F Jaroszyk, M Portalski, Absolute measurement of the thermal conductivity of propylene carbonate by the ac
36 transient hot-wire technique. *Int. J. Thermophys.* **12**, 791–800 (1991).
- 37 5. J Wu, H Zheng, X Qian, X Li, MJ Assael, Thermal conductivity of liquid 1, 2-dimethoxyethane from 243 K to 353 K at
38 pressures up to 30 MPa. *Int. J. Thermophys.* **30**, 385–396 (2009).
- 39 6. DG Cahill, Thermal conductivity measurement from 30 to 750 K: the 3ω method. *Rev. Sci. Instruments* **61**, 802–808
40 (1990).